Improving the Value of EO-1 Observations

Mark Abramson, David Carter, Brian Collins, Stephan Kolitz, Pete Scheidler, Charles Strauss
The Charles Stark Draper Laboratory, Inc.
Cambridge, MA 02139

Abstract:

We have used Draper Lab's Earth Phenomena Observing System testbed ability to utilize near-real-time cloud cover data generated by processing data produced by the Air Force Weather Agency's Stochastic Cloud Forecast Model. The cloud cover data is used as input for the EPOS planner in the tasking of the Hyperion instrument on EO-1, with the objective of achieving increased value of the observation data. The cloud cover data includes forecasts provided every six hours for 3-hour periods up to 84 hours in the future.

We describe the process used to generate the recommended target for Hyperion to image. The recommendation is sent to EO-1 operations in time for the command to be uplinked to EO-1. We present the results of a number of experiments using this capability.

I. Introduction

We have used Draper Lab's Earth Phenomena Observing System testbed ability to utilize near-real-time cloud cover data generated by processing data produced by the Air Force Weather Agency's (AFWA) Stochastic Cloud Forecast Model (SCFM). The cloud cover data is used as input for the EPOS planner in the tasking of the Hyperion instrument on EO-1, with the objective of achieving increased value of the observation data. The cloud cover data includes forecasts provided every six hours for 3-hour periods up to 84 hours in the future.

While the focus here is on describing how we support EO-1 observations, we also include a more general description of the capabilities of EPOS.

II. EPOS Concept of Operations

Variations of the basic EPOS Concept of Operations have been described in previous ESTC papers. The basic concept of operations is to use observation data gathered from one or more space-based sensors to cue the dynamic replanning and tasking of other space-based sensors. For EO-1 missions operations, we provide cloud coverage estimates to improve the chances of cloud-free imaging of targets.

III. EPOS

A. *EPOS Architecture*

There are five components in the EPOS architecture, as illustrated in Figure 1.

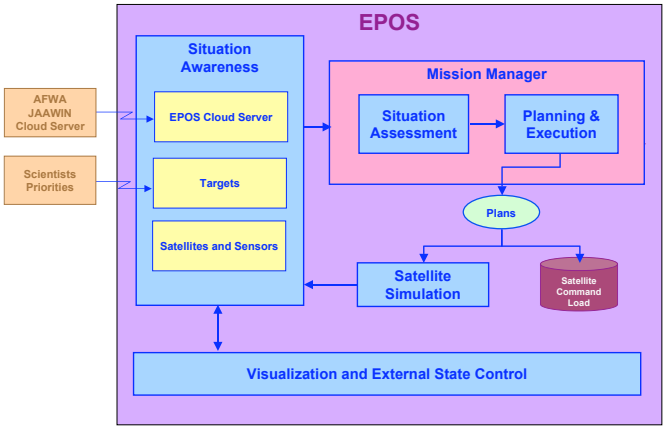

Figure 1: EPOS System Architecture

- **Situation Awareness.** Situation Awareness of the state of the world occurs through External State Servers. These servers are queried by Situation Assessment. One of the external state servers is the AFWA cloud server; it is accessed through the EPOS Cloud Server. For the EO-1 application described below, an external state server is the target list generation process. This process has been mostly manual but is evolving into one that will be largely automated
- **Situation Assessment.** Situation assessment propagates satellites, identifies candidate targets, and generates a target-value table that will be used by Planning and Execution.
- **Planning and Execution**. Planning and Execution generates the plan from information passed by Situation Assessment and passes the plan appropriately to the simulation or a real-world system.
- **Satellite Simulation**. Satellite Simulation executes the plan and in turn updates the external state.
- **Visualization and External State Control.** Visualization and External State Control is used by the user to monitor the progress of the simulation and to modify the external state in Situation Awareness.

B. SITUATION AWARENESS

Cloud Data

We start with data provided by AFWA's Stochastic Cloud Forecast Model for cloud cover forecasting and decision-making in EPOS. The model uses observed cloud data from five geosynchronous and four polar orbiting satellites. AFWA's cloud forecast system provides hemispheric polar-stereographic grids in Gridded Binary format at six-hour intervals. The data is provided in polar-stereographic grids of 1024 by 1024 for each hemisphere with cells having a rectangular dimension of approximately 24 km at ±60° latitude. Cloud forecasts are generated at 00Z, 06Z, 12Z and 18Z. Each forecast contains 56 files; one forecast file for each hemisphere for every 3-hour period in an 84 hour forecast duration. Cloud amounts are expressed in percentages to the nearest 1%, The cloud forecast is available on the Air Force Weather Agency's FTP server some time after the generation times and are available on the EPOS Cloud Server approximately 1.5 hours after the generation times.

Target List

The target list for EO-1, illustrated in Figure 2, is provided weekly in the form of a table. The format has changed in recent months, but the following figure illustrates the basic information. The primary target is marked with a single x, while a secondary target is marked with a double xx. The satellite is operated to optimize the quality of the image of the primary target. Telemetry, Tracking, and Command (TT&C) messages occur at an SB Pass, while downloading of the image data and subsequent reinitialization of the onboard data storage occurs at an XB Pass.

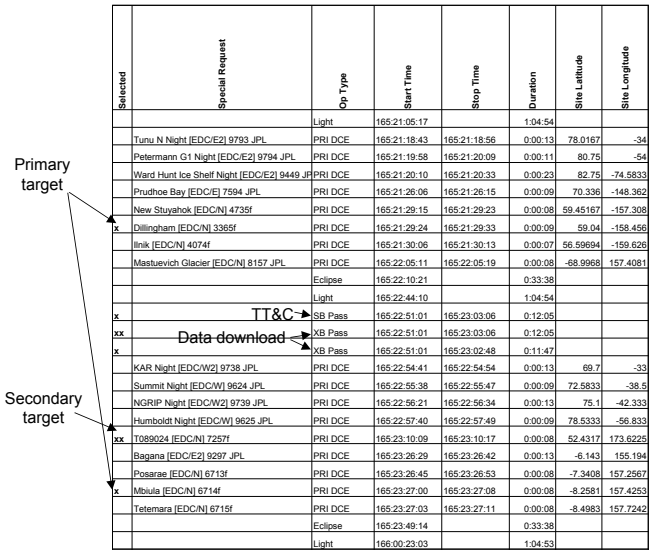

Selected	Special Request	Op Type	Start Time	Stop Time	Duration	Site Latitude	Site Longitude
		Light	165:21:05:17		1:04:54		
	Tunu N Night [EDC/E2] 9793 JPL	PRI DCE	165:21:18:43	165:21:18:56	0:00:13	78.0167	-34
	Petermann G1 Night [EDC/E2] 9794 JPL	PRI DCE	165:21:19:58	165:21:20:09	0:00:11	80.75	-54
	Ward Hunt Ice Shelf Night [EDC/E2] 9449 JP	PRI DCE	165:21:20:10	165:21:20:33	0:00:23	82.75	-74.5833
	Prudhoe Bay [EDC/E] 7594 JPL	PRI DCE	165:21:26:06	165:21:26:15	0:00:09	70.336	-148.362
	New Stuyahok [EDC/N] 4735f	PRI DCE	165:21:29:15	165:21:29:23	0:00:08	59.45167	-157.308
x	Dillingham [EDC/N] 3365f	PRI DCE	165:21:29:24	165:21:29:33	0:00:09	59.04	-158.456
	Ilnik [EDC/N] 4074f	PRI DCE	165:21:30:06	165:21:30:13	0:00:07	56.59694	-159.626
	Mastuevich Glacier [EDC/N] 8157 JPL	PRI DCE	165:22:05:11	165:22:05:19	0:00:08	-68.9968	157.4081
		Eclipse	165:22:10:21		0:33:38		
		Light	165:22:44:10		1:04:54		
x		SB Pass	165:22:51:01	165:23:03:06	0:12:05		
xx		XB Pass	165:22:51:01	165:23:03:06	0:12:05		
x		XB Pass	165:22:51:01	165:23:02:48	0:11:47		
	KAR Night [EDC/W2] 9738 JPL	PRI DCE	165:22:54:41	165:22:54:54	0:00:13	69.7	-33
	Summit Night [EDC/W] 9624 JPL	PRI DCE	165:22:55:38	165:22:55:47	0:00:09	72.5833	-38.5
	NGRIP Night [EDC/W2] 9739 JPL	PRI DCE	165:22:56:21	165:22:56:34	0:00:13	75.1	-42.333
	Humboldt Night [EDC/W] 9625 JPL	PRI DCE	165:22:57:40	165:22:57:49	0:00:09	78.5333	-56.833
xx	T089024 [EDC/N] 7257f	PRI DCE	165:23:10:09	165:23:10:17	0:00:08	52.4317	173.6225
	Bagana [EDC/E2] 9297 JPL	PRI DCE	165:23:26:29	165:23:26:42	0:00:13	-6.143	155.194
	Posarae [EDC/N] 6713f	PRI DCE	165:23:26:45	165:23:26:53	0:00:08	-7.3408	157.2567
x	Mbiula [EDC/N] 6714f	PRI DCE	165:23:27:00	165:23:27:08	0:00:08	-8.2581	157.4253
	Tetemara [EDC/N] 6715f	PRI DCE	165:23:27:03	165:23:27:11	0:00:08	-8.4983	157.7242
		Eclipse	165:23:49:14		0:33:38		
		Light	166:00:23:03		1:04:53		

Figure 2: Initial Portion of EO-1 Target List

C. SITUATION ASSESSMENT

LOS/FOV Value Calculation

We use the cloud coverage data as input in the calculation of the value of observations with a given line of sight/field of view (LOS/FOV). For limb observations, the LOS intersects a number of cloud cells. At 60° latitude, this translates into approximately 15 cells that are traversed. For near-nadir observations, such as those done using EO-1's Hyperion sensor, the LOS/FOV typically intersects only one cell.

We integrate the percentage cloud coverage in each cell over the portion of each cell in the LOS/FOV to calculate a total cloud coverage measure for the LOS/FOV. This integrated cloud coverage is multiplied by the intrinsic target scientific value taken from scientists' priorities. For example, if there is a value of 100 for a sensor to observe a particular target without clouds, and a cloud density of 0.5 (50%), the value is reduced to 50.

Figure 3 illustrates the LOS/FOV projection for a limb sounding sensor, the red line close to the satellite ground track.

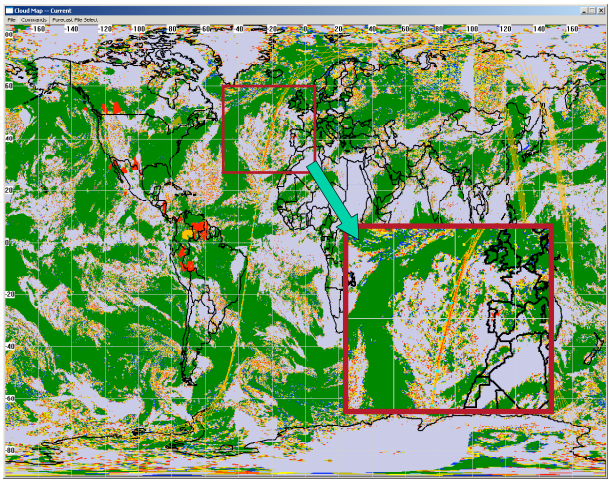

Figure 3. World with Cloud, Satellite Track and Chosen LOS/FOV

Satellite Orbital Propagation

We have software implemented to propagate EO-1's orbit and calculate the times at which Hyperion can observe targets. We initialize with EO-1's NORAD TLE set and a list of EO-1 targets. We use J_2 theory to propagate the NORAD TLE to the first descending equator crossing, corresponding to a particular coordinate in the WRS (world reference system). From that point on, we propagate from WRS grid point to WRS grid point, incrementing time by the orbital period / 248 (the number of grid points per revolution). This method produces results that match the information in the EO-1 target list, which includes observation start and stop stops. EPOS

also has the ability to propagate EOS satellites' orbits independent of the WRS.

D. MISSION MANAGER

We describe two approaches to optimized sensor tasking, the first for a moded sensor, the second focused on EO-1.

Optimized Modal Sensor Tasking

In this section, we formulate an optimization approach to automated task planning of moded sensors such as HIRDLS and TES. For such a sensor, the task plan is a *schedule,* a time-tagged sequence of mode commands (t_1,m_1), (t_2,m_2), …, (t_r,m_r). Interpretation: "Command mode m_1 at time t_1, then command mode m_2 at time t_2, and so forth."

Often a mode corresponds to a scan pattern in the sensor pointing angles. (For HIRDLS, these are azimuth and elevation.) Modes will thus have associated *durations;* we denote the duration of mode m by $\tau(m)$. It will generally be the case that we intend modes to run to completion: it is natural to think of the sequence t_1, t_2, …, t_r of times associated to a task plan as monotonically increasing, and we shall typically assume that $t_{i+1} - t_i \geq \tau(m_i)$ for all i between 1 and $r - 1$. In any real application $\tau(m)$ will be positive for every mode m.

It won't be unusual to plan multiple consecutive occurrences of the same mode. The TES Global Survey Mode, for example, has period 81.2 seconds, and it is intended that this mode operated continuously for approximately a day, e.g., for 16 consecutive orbits (1568 minutes, about 10 percent longer than 1 day). We would represent such a schedule by a sequence of the form (t_1,m), (t_2,m), …, (t_r,m) where m is TES Global Survey Mode and $t_{i+1} - t_i = \tau(m) = 81.2$ sec for all i between 1 and $r - 1$.

The abstract sensor task-planning problem:

Let $T - [t_0, t_f]$ be a finite closed interval, called the *planning interval.*

Let M be an arbitrary set whose elements are called *modes*.

Let v be a real-valued function on $T \times T \times M$. The real number $v(t, t', m)$ is called the *value* associated with (re)starting mode m at time t, and maintaining until time t'. We will be most interested in the case $t' - t = \tau(m)$.

For each j in a finite index set J, let C_j be a nonnegative real-valued function on $T \times T \times M$ and let C_j be a nonnegative real number. We interpret $C_j(t, t', m)$ as a quantity of *resource of type j* which is consumed by (re)starting mode m at time t, and maintaining until time t'. C_j is the total amount of this resource available for the planning interval.

Let N_{max} be a positive integer.

Select N between 1 and N_{max}, a sequence of modes $m_1, m_2, \ldots, t_N$, and an associated sequence of times $t_1, t'_1, t_2, t'_2, \ldots, t_N, t'_N$ with $t_0 \leq t_1 < t'_1 \leq t_2 < t'_2 \leq \ldots \leq t_N < t'_N \leq t_f$ to *maximize*

$$V = \sum_{i=1}^{N} v(t_i, t'_i, m_i)$$

subject to the constraints (for j *in* J*)*

$$\sum_{i=1}^{N} c_j(t_i, t'_i, m_i) \leq C_j$$

In our application, the mode set M and the value function V depend implicitly on the *satellite,* its *ephemeris,* and the *sensor*. Value $v(t_i, t'_i, m_i)$ depends on times t_i and t'_i because of the motion of the satellite relative to the set of targets that have scientific value for observation. The value for each target is also modified by forecast cloud coverage in the LOS/FOV from the sensor to the target.

The restricted sensor task planning problem:

An important special case of the abstract sensor task-planning problem can be recast as a graph-theoretic optimization. We impose the following assumptions for now:

Mode transition times are chosen from a discrete subset T_0 of the planning interval T.

There is a distinguished element ϕ of M called the *idle mode* whose duration $\tau(\phi)$ is arbitrarily small. (This technical condition makes ϕ easy to schedule.)

A mode, if scheduled, runs to completion. The instrument is idle from the time of mode completion until the next available transition time.

The resource constraint set J is empty, i.e., there are no resource (e.g., data storage, power) constraints.

Select N*, a sequence of modes* $m_1, m_2, \ldots, m_N$*, and an associated sequence of times* $t_1, t_2, \ldots, t_N$ *from the discrete set* T_0 *to maximize*

$$V = \sum_{i=1}^{N} v(t_i, t_i + \tau(m_i), m_i)$$

subject to the constraints

$$t_0 \leq t_1$$
$$t_i + \tau(m_i) \leq t_{i+1} \qquad \text{(for } i = 1, 2, \ldots, N\text{-}1\text{)}$$
$$t_N + \tau(m_N) \leq t_f$$

Associate to this problem a weighted directed acyclic graph G as follows:

Vertices of G are ordered pairs (t, m) where t is in T_0 and m is in M.

There is an edge from (t, m) to (t', m') whenever t' is the smallest element of T_0 for which $t + \tau(m) \leq t'$

An edge from (t, m) to (t', m'), when it exists, is given negative weight $-v(t, t + \tau(m), m)$.

A solution to the restricted sensor-scheduling problem is just a shortest path in G.

Figure 4 illustrates the modal sensor task planning optimization formulated as a shortest path problem through an acyclic graph whose nodes are (time, mode) pairs with arcs representing feasible mode transitions. The arc from (t_1, m_1) to (t_2, m_2) represents mode m_1 starting at time t_1, followed by mode m_2 starting at time t_2. The difference between t_2 and t_1 is greater than the duration required to completely execute mode m_1. The cost along the arc is the negative of the value gained from starting mode m_1 at time t_1.

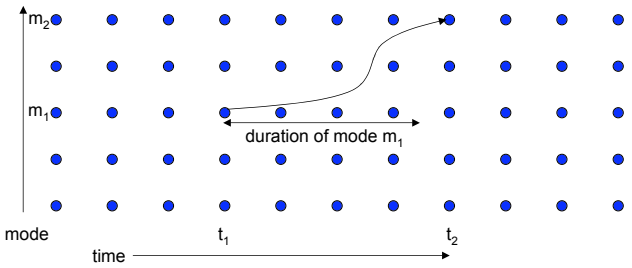

Figure 4: Acyclic Graph for Optimized Modal Sensor Tasking

Scheduling Graphs: An Efficient Algorithm

We used a straightforward algorithm to solve the shortest path problem taken from chapter 25 of T. Cormen, C. Leiserson, and R. Rivest, *Introduction to Algorithms,* The MIT Press, (23rd printing), 1999.

Let G be a weighted directed acyclic graph. A topological ordering of the vertices of G is a partial order with the property that U precedes U' whenever there is an edge from U to U'. The scheduling graph introduced in the previous section is topologically ordered; vertex (t, m) precedes vertex (t', m') whenever $t < t'$.

A shortest path in a topologically ordered directed acyclic graph with n vertices and e edges and a unique source vertex u_0 (a vertex which is smallest in the topological ordering) can be determined in time O(n+e) using the following algorithm (*ibid.,* p. 536):

```
set d[u0] to 0
for each vertex u not equal to u0{
        set d[u] to infinity
        set predecessor[u] to nil
}
for each vertex w taken in topologically
sorted order {
        for each vertex w adjacent to u {
        if d[u] > d[w] + weight(w,u) {
        set d[u] to d[w] + weight(w,u)
        set predecessor[u] to w
        }
        }
}
```

This algorithm depends critically on acyclicity of G. It works even if there are negative edge weights; in our application all edge weights are negative. In an example with 5 modes (including idle), with mode durations between 27 and 93 seconds, and a planning horizon of 90 minutes (5400 seconds), there were 27,005 nodes and approximately 135,000 edges. Solution time for the optimization was 47 milliseconds on a 3.2 GHz Pentium 4 running Windows XP.

Planning EO-1 Imaging Using EPOS

In the preceding, imaging start and end times were variables, to be selected as part of the optimization. In EO-1 operations, image start and end times are constrained. To make EPOS processing compatible with this, we have reformulated the optimization problem and written new solver software. We describe here the EO-1 optimization problem and how the technique of dynamic programming is applied to solve it.

Before stating the optimization problem, it is helpful to describe astrodynamic modeling that can be done in advance. We obtain the EO-1 ephemeris and the following information from the EO-1 target list:

- Site latitude
- Site longitude
- Desired time at start of imaging
- Desired time at end of imaging

Using this information, it is possible to compute coordinates of the line-of-sight vector from spacecraft to target at the midpoint of the imaging interval. From the line of sight vector, we can infer pointing angles x (roll) and y (pitch) at imaging midpoint. Presently we *assume* that these pointing angles remain constant from time at start of imaging to time at end of imaging, but our optimization formulation permits pointing angles to change during the imaging period.

It's important to note, though, that initial astrodynamic modeling permits us to assume that the following information is available for each candidate target:

- Desired time at start of imaging

- Initial pointing angles
- Desired time at end of imaging
- Final pointing angles

A feasible imaging schedule must allow sufficient time for spacecraft slew between end of imaging on a selected target and start of imaging on the next selected target. We take this into account in the optimization problem formulation below.

The Formal EO-1 Optimization Problem

The problem is to choose targets to be imaged from a list which is provided.

Each target i is an 8-tuple (t_i , x_i , y_i , t_i' , x_i' , y_i' , r_i , v_i). t_i is time at which imaging of i would commence, t_i' is time at which imaging of i would end, x_i and y_i are initial pointing angles, x_i' and y_i' are final pointing angles, r_i is resource needed (e.g., for data storage), and v_i is the value of imaging target i.

Our job is to choose a subsequence S of largest total value, subject to a resource constraint:

$$\sum_{i \in S} r_i \le R$$

and to *slewing constraints:* If i and j are consecutive elements of S, we require that

$$|x_j - x_i'| \le (t_j - t_i' - \sigma)s_x$$
$$|y_j - y_i'| \le (t_j - t_i' - \sigma)s_y$$

Constants s_x and s_y are slew rate bounds; σ is a constant called settling time.

Solving The EO-1 Problem By Dynamic Programming

To solve this problem by dynamic programming, let q denote system *state;*

q is a 4-tuple (t, x, y, r) where x and y are pointing angles which occur at time t, and r is resource available.

We say that target i = (t_i , x_i , y_i , t_i' , x_i' , y_i' , r_i , v_i) is *feasible* from q = (t, x, y, r), and write i | q if the following four conditions hold:

$$t_i \le t$$
$$r_i \le r$$
$$|x_i - x| \le (t_i - t - \sigma)s_x$$
$$|y_i - y| \le (t_i - t - \sigma)s_y$$

Each state q has *value* V(q); this is the largest total value we can obtain by scheduling targets if the initial state is q. Bellman's equation, also called the *principle of optimality* allows value to be determined recursively. If there are no targets i which are feasible from q, V(q) = 0. Otherwise, we have

$$V(q) = \max_{i|q} (v_i + V(q^i))$$

where the state q^i is defined as follows:

$$q^i = (t_i', x_i', y_i', r - r_i)$$

Notice that the *first* target in an optimal schedule is the i which maximizes in the equation above for V(q). Subsequent targets are found in the course of the recursion that that equation represents.

The techniques just summarized have been implemented in software and tested in simulation.

E. VISUALIZATION

The EPOS WorldDisplay presents a Mercator projection of the Earth (including e.g., administrative boundaries, rivers), targets, satellite ground tracks, and cloud cover. It can be used to generate single images or a series of images as a movie. It can: assemble, store on disk, and display any sequence of forecast or current cloud maps, run movies at different speeds, single frame step forward or backward, show a full world map display or zoomed display, show the EO-1 swath of potential views, i.e., an optional display of 2.5 WRS swath on either side of the nadir track of EO-1, show EO-1 targets within this swath, select starting longitude choice facility (for easier selection of areas and targets near sides of the full world map), display target names, locations and cloud cover, assemble, store on disk, display comparisons through time of current and forecast cloud maps in a side-by-side view, and display a movie of differences between two frames, e.g., actual and forecast for the same time period. It can convert movies to AVI format and save them as files.

The first frame of an example side-by-side movie is shown in Figure 5.

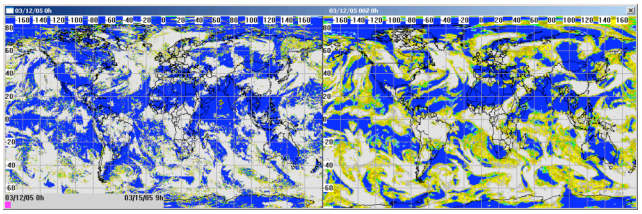

Figure 5: First Frame of Side-By-Side Movie (actual on left, forecast on right)

TV Guide

A new display is being developed to highlight the opportunities for simultaneous or near-simultaneous viewing of a target from multiple satellite sensors. This display has the form of an extended scrollable time line and is modeled on the familiar TV Guide at-a-glance chart that indicate what shows are on what channels at what time. This chart is optionally synchronized with STK, so the positions and sightings of the chosen satellites at any

time can be displayed in 3D in an STK window. Figure 6 illustrates a notional case. The sensor models used for this development are stubbed notional ones. We have modeled in detail a subset of the ones in the figure.

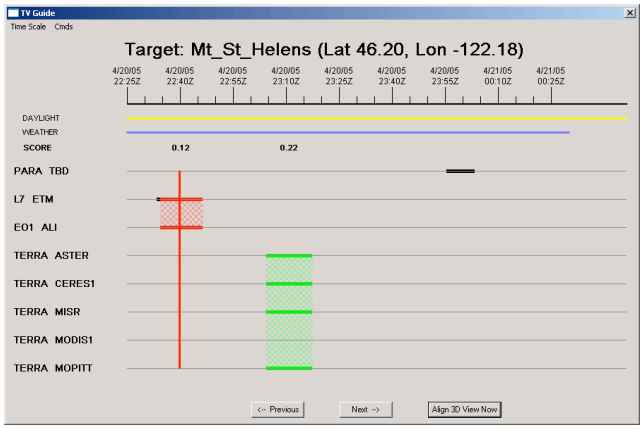

Figure 6: Example TV Guide Display

IV. Application to EO-1 Operations

Operational Considerations

Cloud forecasts are generated every six hours at 00Z, 06Z, 12Z and 18Z. Each forecast contains 56 files; one forecast file for each hemisphere for every 3-hour period in an 84 hour forecast duration. The cloud forecast is available on the Air Force Weather Agency's FTP server some time after the generation times and are available on the EPOS Cloud Server approximately 1.5 hours after the generation times.

We have conducted a number of experiments during EO-1 operations, suggesting which target to actually image, based on cloud cover. In the first six experiments that were performed, five resulted in the proper target selection. Four resulted in a pick that had less cloud cover than the original selection that was made in the current EO-1 target selection process that does not use a cloud cover forecast. Starting with the third test on December 15, 2004, the process of ingesting the EPOS cloud cover forecast was automated on the NASA side. Table 1 summarizes the six tests. Our own testing of the forecasts on a set of targets indicates that the results of the table are better than what can normally be expected. The benefit of using the cloud forecasts over time is still clear based on our more extensive testing. More details on the results of these tests will be presented at ESTC 2005.

Date	Target name	latitude	longitude	Realized % cloud cover	Forecast lead time (hours)	Original selection (x primary xx secondary	Selected by EPOS
12/1/2004					9		
	Oil Creek	57.684	-155.724	46%		x	
	T070073	-19.7444	-175.0778	0%			x
12/7/2004					16		
	Bishnupur	25.8833	91.2	47%		x	
	Netrokoma	24.55	90.71667	0%			x
12/15/2004					15		
	Kunming	25.05472	102.6856	46%			
	Ban Kok Pho	17.41222	101.3064	0%		x	x
	Kutabuluhpasar	3.04028	98.145	100%			
12/22/2004					3		
	T089024	52.4317	173.6225	100%			
	Posarae	-7.3408	157.2567	0%			x
	Mbiula	-8.2581	157.4253	14%		x	
1/28/2005					3-5		
	T09212	68.28028	-179.3386	0%			
	Mayno-Gytkino	63.4644	176.5231	0%			x
	Colleambally	-34.8012	146.0136	83%		x	
2/4/2005					12-14		
	Kait	-4.44583	152.6608	91%		xx	x
	Emerald	-23.52472	148.1414	0%			
	Melbourne NP	-37.4823	114.4035	66%		x	

Table 1: EO-1 EPOS Initial Experiments

Subsequent tests have been limited due to a variety of factors, including a significant change in how observation planning is done for EO-1 from a mostly manual process to one that will be largely automated.

Acknowledgments

This material is based upon work supported by the National Aeronautics and Space Administration's AIST program, under Contract #NAS5-03121, through the Goddard Space Flight Center. Any opinions, findings, and conclusions or recommendations expressed in this paper are those of the authors and do not necessarily reflect the views of the National Aeronautics and Space Administration